

## Asymmetry and Dynamics in Bis-intercalated DNA

Mary Elizabeth Peek,<sup>a</sup> Leigh Ann Lipscomb,<sup>a</sup> John Haseltine,<sup>a</sup> Qi Gao,<sup>b</sup> Bernard P. Roques,<sup>c</sup>  
 Christiane Garbay-Jaureguiberry<sup>c</sup> and Loren Dean Williams<sup>a\*</sup>

<sup>a</sup>School of Chemistry and Biochemistry, Georgia Institute of Technology, Atlanta, GA 30332-0400 U.S.A.

<sup>b</sup>Department of Analytical Chemistry, Bristol-Myers Squibb Company, Wallingford, CT 06492 U.S.A.

<sup>c</sup>Département de Chimie Organique U266 INSERM, URA D1500 CNRS des Sciences Pharmaceutiques et Biologiques,  
 4 Avenue de l'Observatoire, 75006 Paris, France

**Abstract**—The bis-intercalator ditercalinium (NSC 366241), composed of two 7H-pyridocarbazoles linked by a bis(ethylpiperidinium), binds to DNA with a binding constant greater than  $10^7 \text{ M}^{-1}$ . One distinctive aspect of the 3-D X-ray structure of a DNA–ditercalinium complex is its asymmetry. We propose here that the activity of ditercalinium may be related to structural polymorphism and dynamic conversion between conformers. It was previously reported that activity is closely related to linker composition. Activity increases with increasing conformational restraints of the linker. We suggest these conformational restraints can lead to asymmetry in DNA complexes and that this asymmetry results directly in structural polymorphism. Using the Cambridge Structural Database (CSD) as a source of information about chemical fragments that are analogous to the linker of ditercalinium, we have explored the conformational space available to ditercalinium. The results indicate that the linker is highly constrained and that the DNA complex is intrinsically asymmetric. We propose a reasonable mechanism of ring reversal that is consistent with the conformations of analogous fragments within the CSD.

### Introduction

Affinity for DNA is a common characteristic of compounds with antitumor activity. In part because of their high DNA affinity,<sup>1,2</sup> bis-intercalators are attractive chemotherapeutic prospects. The bis-intercalator ditercalinium (NSC 366241, Fig. 1A), composed of two 7H-pyridocarbazoles linked by a bis(ethylpiperidinium), binds to DNA with a binding constant greater than  $10^7 \text{ M}^{-1}$ .<sup>3</sup> Ditercalinium possesses antineoplastic activity<sup>4</sup> and at one point reached clinical trials. The mode of action of this compound is unique among non-covalent DNA binding agents: it induces malfunction of DNA repair systems.<sup>5–8</sup>

One distinctive aspect of the 3-D X-ray structure of a DNA–ditercalinium complex<sup>9,10</sup> is its asymmetry. This asymmetry was not anticipated. The DNA and the drug alone are both symmetric. Ditercalinium is a symmetrical dimer and the DNA is a self-complementary duplex, [d(CGCG)]<sub>2</sub>. In the X-ray structure, one linker nitrogen (N-21) of ditercalinium forms a hydrogen bond to an N-7 position of a guanine. A second guanine N-7, related to the first by pseudo two-fold symmetry, has no hydrogen bonding partner. Instead, the proton of the second linker nitrogen (N-21'), related to the first by pseudo two-fold symmetry, is directed away from the DNA toward the solvent region. As we have described,<sup>11</sup> asymmetry of the linker causes asymmetry of the DNA. The hydrogen bond at one end of the complex effectively pulls one base pair toward the major groove.

We propose here that the activity of ditercalinium may be related to structural polymorphism and dynamic

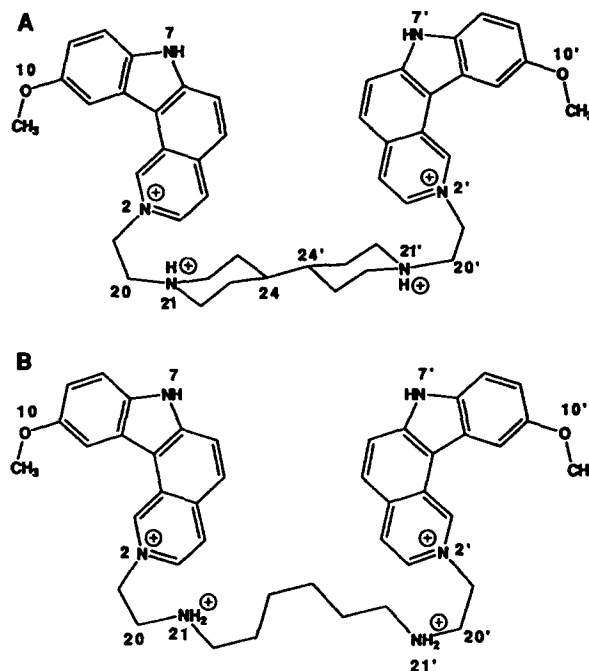
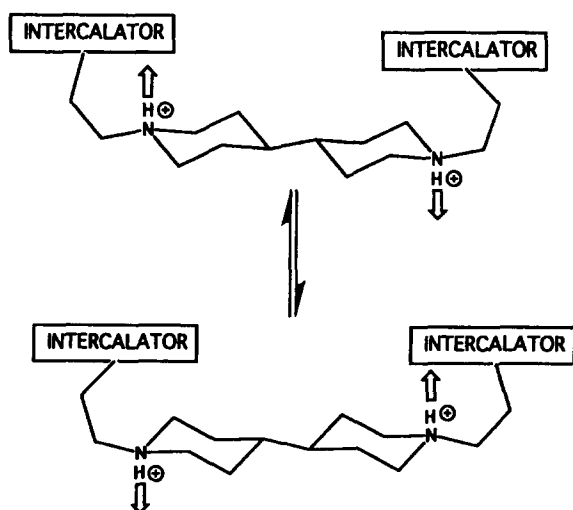


Figure 1. (A) Ditercalinium, and (B) Flexi-Di.

conversion between conformers. It was previously reported that activity is closely related to linker composition.<sup>12,13</sup> Activity increases with increasing conformational restraints of the linker. We suggest that these conformational restraints can lead to asymmetry in DNA complexes and that this asymmetry results in structural polymorphism. The conformational space of this type of asymmetric complex contains degenerate states. Therefore, the complexes should be dynamic, converting

between these states. In the case of ditercalinium the asymmetry of the DNA complex results in two isoenergetic complexes interconverted by reversal of the relative orientations of the piperidinium rings. Ring reversal can be achieved by net rotation of the linker about its long axis (Fig. 2). The conformation of the DNA at each end of the complex similarly interconverts. We propose a dependence of activity on asymmetry and dynamics. The unusual activity of ditercalinium may ultimately be related to the dynamic nature of its complexes with DNA.



**Figure 2.** Schematic representation of ring reversal. Arrows represent the directions of the N–H bonds of the linker. In the ditercalinium–[d(CGCG)]<sub>2</sub> complex, the linker proton labeled with an up arrow forms a hydrogen bond to the DNA and that labeled with a down arrow is directed out toward the solvent region. Ditercalinium appears to form a dynamic complex with DNA, converting between isoenergetic states.

Each analog of ditercalinium that is active in eukaryotes is observed or predicted to form an asymmetric complex with DNA. Conversely each inactive analog is observed or predicted to form a symmetric complex. For example, Flexi-Di<sup>12</sup> (Fig. 1B) forms a relatively symmetric complex with DNA and is inactive. Flexi-Di is composed of two 7*H*-pyridocarbazoles linked by a flexible, spermine-like linker of the same length and charge distribution as ditercalinium. A lack of conformational restraints of the linker facilitates symmetry in this DNA complex. In the crystal structure of a DNA–Flexi-Di complex,<sup>11</sup> protons of both linker nitrogen atoms are directed toward the DNA such that each linker nitrogen of Flexi-Di forms a hydrogen bond to an N-7 position of a guanine. This symmetric complex, with one energetic minimum, is expected to be static. Insertion of a methylene between the two piperidinium groups of ditercalinium maintains asymmetry (model building, unpublished) and activity.<sup>13</sup> In contrast, insertion of an ethylene between the two piperidinium groups abolishes asymmetry (model building, unpublished) and activity.<sup>13</sup>

Here we describe the structural basis for asymmetry of the ditercalinium complex. Using the Cambridge Structural Database (CSD) (5.07, April 1994)<sup>14</sup> as a source of information about chemical fragments that are analogous to the linker of ditercalinium, we have characterized the

conformational space available to ditercalinium. The results indicate that the linker is highly constrained and that the DNA complex is intrinsically asymmetric. We propose a reasonable mechanism of ring reversal that is consistent with the conformations of analogous fragments within the CSD.

## Results

We have employed the CSD as a source of information about the conformation of the linker of ditercalinium. The crystal structure of ditercalinium alone has not been reported. However, many structures of molecules that are analogous to ditercalinium are contained in the CSD. Two classes of molecules are defined here. Class I fragments (Fig. 3A) are single ring systems and Class II fragments (Fig. 3B) are dual ring systems.

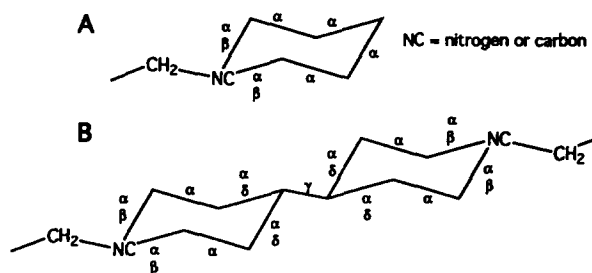


**Figure 3.** Schematic diagram of CSD search fragments. (A) Class I fragment, and (B) Class II fragment. Torsion angles are labeled at the central bond. Endocyclic torsion angles are denoted by  $\alpha$ . Exocyclic torsion angles involving a methylene substituent are denoted by  $\beta$  and indicate the axial or equatorial position of the methylene substituent. Exocyclic torsion angles with three atoms from one ring and the fourth from the second ring are denoted by  $\delta$  and indicate the equatorial or axial position of the substituent ring. Exocyclic torsion angles involving two atoms from each ring are denoted by  $\gamma$  and indicate the relative rotation of one ring with respect to the other.

As expected,<sup>15,16</sup> each Class I fragment in the CSD is in the chair conformation and each substituent methylene group in the equatorial position. Endocyclic torsion angles are denoted here by the angle  $\alpha(I)$  (Fig. 3A). For simplicity, we have taken the absolute value of each torsion angle described. Although  $\alpha(I)$  is  $60^\circ$  in an ideal chair, this requires C–C–C bond angles of  $109.5^\circ$  rather than the preferred  $112.4^\circ$ . Therefore,  $\alpha(I)$  observed in real chairs is around  $56^\circ$  and C–C–C bond angles are  $111^\circ$ .<sup>17</sup> Twist boat and boat conformations are characterized by certain  $\alpha(I)$  near  $30^\circ$  and  $0^\circ$ , respectively. The observed distribution of  $\alpha(I)$  is shown in Figure 4A. The distribution of 282 torsion angles  $\alpha(I)$  is nearly Gaussian and averages  $55.6^\circ$ . The range is from  $50.9^\circ$  to  $60.4^\circ$  ( $\sigma = 1.94^\circ$ ). Thus all 47 Class I fragments are in the chair conformation. No examples of boat or twist boat conformations are observed. Exocyclic torsion angles involving the methylene group are denoted by  $\beta(I)$  (Fig. 3A). For equatorial conformers  $\beta(I)$  is expected to be around  $180^\circ$  and for axial conformers around  $60^\circ$ . The observed distribution of  $\beta(I)$  is shown in Fig. 4B. The torsion angle  $\beta(I)$  averages  $179.9^\circ$  and is always greater in absolute value than  $171^\circ$  ( $\sigma = 3.01^\circ$ ). No examples of axial methylene groups in Class I fragments were observed.

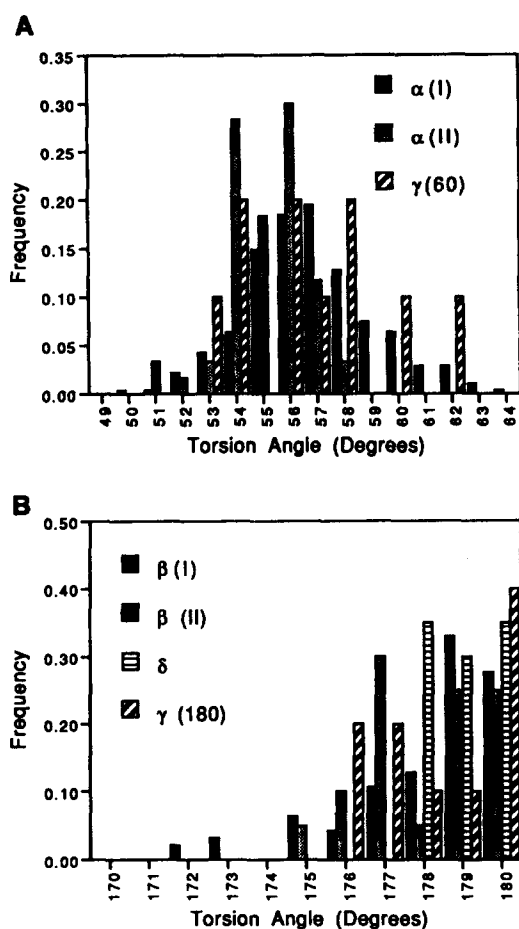


**Figure 4.** Frequency distribution of torsion angles of CSD entries containing Class I and II fragments. Absolute values of torsion angles were used for the analysis described here. Distributions of torsion angles, in increments of one degree, were calculated and normalized. (A) Endocyclic torsion angles for Class I molecules [ $\alpha$ (I)] are black and for Class II molecules [ $\alpha$ (II)] are gray. Exocyclic torsion angles  $\gamma$  near  $60^\circ$  [ $\gamma$ (60)] are diagonal lines. All torsion angles for  $\alpha$ (I),  $\alpha$ (II), and  $\gamma$ (60) lie between  $49^\circ$  and  $64^\circ$ . There are 282  $\alpha$ (I), 60  $\alpha$ (II), and 10  $\gamma$ (60) torsion angles. (B) Exocyclic torsion angles  $\beta$  for Class I molecules [ $\beta$ (I)] are black,  $\beta$  for Class II molecules [ $\beta$ (II)] are gray,  $\delta$  are horizontal lines, and  $\gamma$  near  $180^\circ$  [ $\gamma$ (180)] are diagonal lines. All torsion angles for  $\beta$ (I),  $\beta$ (II),  $\delta$ , and  $\gamma$ (180) lie between  $170^\circ$  and  $180^\circ$ . There are 94  $\beta$ (I), 20  $\beta$ (II), 20  $\delta$ , and 10  $\gamma$ (180) torsion angles.

Each Class II fragment is in a dual chair conformation with ring substituents in equatorial positions. Endocyclic torsion angles of each Class II fragment are denoted by  $\alpha$ (II) (Fig. 3B). The observed distribution is shown in Figure 4A. The torsion angle  $\alpha$ (II) averages  $54.6^\circ$  and ranges from  $50.8^\circ$  to  $57.4^\circ$  ( $\sigma = 1.49^\circ$ ). Exocyclic torsion angles indicating the position of the methylene substituent are denoted by the angle  $\beta$ (II) (Fig. 3B). For an equatorial substituent  $\beta$ (II) is expected to be  $180^\circ$ , and for an axial substituent  $\beta$ (II) is expected to be near  $60^\circ$ . The observed distribution of  $\beta$ (II) is shown in Figure 4B. For Class II fragments,  $\beta$ (II) averages  $179.9^\circ$  and ranges from  $174.3^\circ$  to  $179.8^\circ$  ( $\sigma = 2.92^\circ$ ). Similarly the exocyclic torsion angle that describes the equatorial/axial position of substituent rings is denoted by torsion angle  $\delta$  (Fig. 3B). An equatorial position is indicated by  $\delta$  near  $180^\circ$ . For Class II fragments  $\delta$  averages  $179.8^\circ$  and ranges from  $177.0^\circ$  to  $180.0^\circ$  ( $\sigma = 1.77^\circ$ ). The observed distribution of

$\delta$  in Class II fragments is shown in Figure 4B. There are no axial substituents in Class II fragments.

Class II fragments could potentially exist as two staggered rotamers along the central bond. The torsion angle describing the rotameric character along the central bond is denoted by  $\gamma$ . One rotamer, termed the  $60_2180_2$  rotamer (Fig. 5A, B), has two torsion angles  $\gamma$  near  $60^\circ$  and two near  $180^\circ$ . The second, termed the  $60_3180_1$  rotamer (Fig. 5C, D), results from a  $120^\circ$  rotation of the  $60_2180_2$  rotamer about  $\gamma$  and has three torsion angles near  $60^\circ$  and one near  $180^\circ$ . Observed angles  $\gamma$  fall exclusively into clusters near  $60^\circ$  and  $180^\circ$  (Fig. 4A, B). Values of  $\gamma$  in the  $60^\circ$  cluster average  $56.4^\circ$  and range from  $52.6^\circ$  to  $61.4^\circ$  ( $\sigma = 2.80^\circ$ ). Values of  $\gamma$  in the  $180^\circ$  cluster average  $178.2^\circ$  and range from  $175.2^\circ$  to  $180.0^\circ$  ( $\sigma = 2.01^\circ$ ). The  $60_3180_1$  rotamer is not observed among Class II fragments but is not expected to be energetically prohibitive. CSD entry VAYXUO, which was screened out ( $\sigma_{c-c} = 0.043 \text{ \AA}$ ) and therefore not included as a Class II fragment, does contain a  $60_3180_1$  rotamer.

Switching N-21 (Fig. 1A) to a carbon has little effect on the conformation of Class I fragments. The geometry of cyclohexane rings is similar to that of piperidinium rings. Among Class I fragments, 15 of the 47 are cyclohexane rings and 32 are piperidinium rings. The average endocyclic torsion [ $\alpha$ (I)] of cyclohexyl Class I fragments [ $55.4^\circ$  ( $\sigma = 1.17^\circ$ )] is similar to that of piperidinium Class I fragments [ $56.7^\circ$  ( $\sigma = 2.59^\circ$ )]. Average C-20 to C-24 distances are similar,  $4.29 \text{ \AA}$  ( $\sigma = 0.04 \text{ \AA}$ ) in cyclohexane rings and  $4.35 \text{ \AA}$  ( $\sigma = 0.03 \text{ \AA}$ ) in piperidinium rings (see Fig. 1 for numbering scheme). Average C-20 to C-21 or C-20 to N-21 distances are similar,  $1.516 \text{ \AA}$  ( $\sigma = 0.004 \text{ \AA}$ ) in cyclohexane rings and  $1.480 \text{ \AA}$  ( $\sigma = 0.003 \text{ \AA}$ ) in piperidinium rings. In addition, the average exocyclic torsion [ $\beta$ (I)] of cyclohexyl Class I fragments [ $178.4^\circ$  ( $\sigma = 1.22^\circ$ )] is similar to that of piperidinium Class I fragments [ $177.4^\circ$  ( $\sigma = 2.14^\circ$ )].

Class I fragments are excellent predictors of Class II conformation. These two classes of fragments are conformationally consistent. Both adopt chair conformations with exocyclic substituents exclusively in equatorial positions. The equatorial link of one ring to another does not alter the conformation of either.

Bis-cyclohexane conformation should be a good predictor of bis-piperidinium conformation. All five Class II fragments contain dual cyclohexane rings (no dual piperidinium rings were extracted from the CSD) so that no direct information on bis-piperidinium conformation was obtained. The predicted correlation between bis-cyclohexane and bis-piperidinium conformation is based on the following observations: (i) mono-cyclic conformation is an excellent predictor of bis-cyclic conformation, and (ii) cyclohexane conformation is an excellent predictor of piperidinium conformation.

The geometry of the linker of ditercalinium in the DNA complex is similar to that observed in Class II fragments. Rings of the linker of ditercalinium adopt the dual

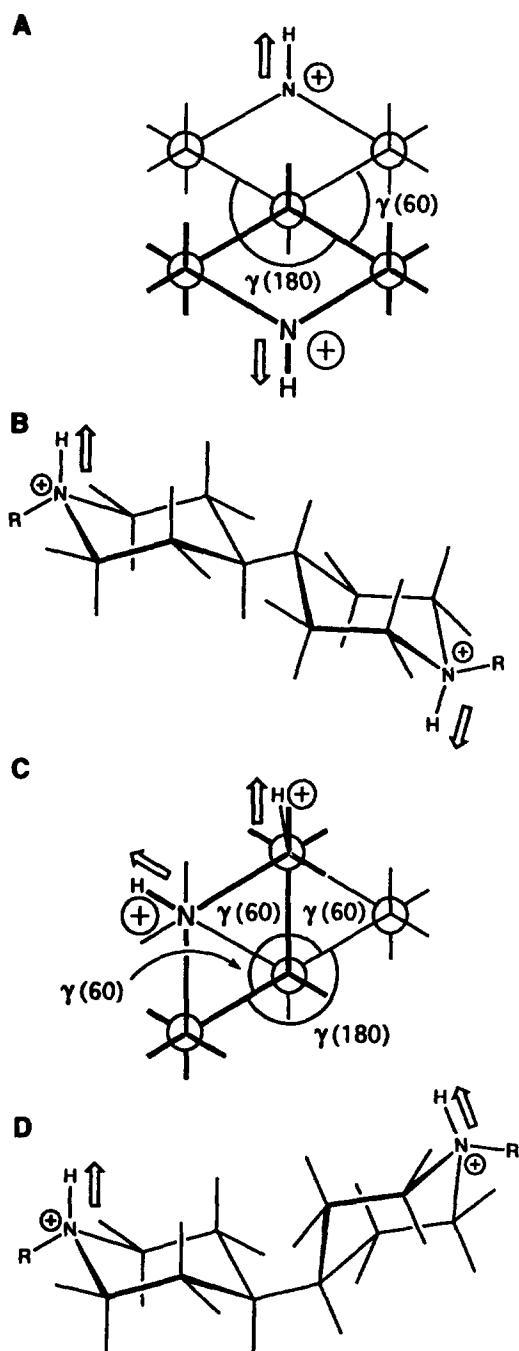


**Figure 5.** Representations of various dual chair conformations of the linker of ditercalinium. Bold lines and larger atoms are nearer to the viewer than thin lines and smaller atoms. Arrows indicate the direction of N-H bonds. Linker protons labeled with up arrows are directed toward the DNA, and those labeled with down arrows are directed away from the DNA. R represents the intercalative group and connecting methylene groups. (A) Newman projection of the  $60_2,180_2$  rotamer. Two of the  $\gamma$  torsion angles that define this rotamer are labeled. (B) Saw horse view of the conformation shown in (A). (C) Newman projection of the  $60_3,180_1$  rotamer. All four  $\gamma$  torsion angles that define this rotamer are labeled. The proton near the vertical arrow has been skewed to the left for clarity. (D) Saw horse view of the conformation shown in (C).

chair/ $60_2,180_2$  rotamer with exclusively equatorial substituents. Endocyclic torsion angles ( $\alpha$ ) for the linker of ditercalinium average  $63.8^\circ$  and range from  $47.1^\circ$  to  $72.7^\circ$  ( $\sigma = 8.04^\circ$ ). Exocyclic torsion angles for  $\beta$  average  $168.5^\circ$  and range from  $155.5^\circ$  to  $179.9^\circ$  ( $\sigma = 10.06^\circ$ ), and

for  $\delta$  average  $170.0^\circ$  and range from  $166.6^\circ$  to  $174.4^\circ$  ( $\sigma = 3.36^\circ$ ). Values of  $\gamma$  are  $50.5^\circ$ ,  $77.9^\circ$ ,  $164.1^\circ$  and  $168.5^\circ$ , giving averages of  $64.2^\circ$  ( $\sigma = 19.40^\circ$ ) and  $166.3^\circ$  ( $\sigma = 3.15^\circ$ ) for the two clusters. The range of endocyclic and exocyclic torsion angles for the linker of ditercalinium is broader than that of either piperidinium or cyclohexyl Class I and II fragments. This dispersion of angles may be due to inaccuracies caused by the relatively low resolution ( $1.7 \text{ \AA}$ ) of the DNA complex in comparison with those of the small molecule entries in the CSD or by DNA-induced conformational distortion.

The conformation of the dual ring system of Class II fragments is highly constrained. As a result of these constraints, in the five examples extracted from the CSD, the range of the distances between methylene carbon atoms (corresponding to the C-20-C-20' distance of ditercalinium) is small, with a minimum  $10.23 \text{ \AA}$  and a maximum  $10.27 \text{ \AA}$  (mean =  $10.25 \text{ \AA}$ ,  $\sigma = 0.02 \text{ \AA}$ ). The observed C-20-C-20' distance in the ditercalinium complex is considerably less,  $9.70 \text{ \AA}$ . In spite of the constraints of the bis(ethylpiperidinium) ring system, in ditercalinium this system is compressed relative to that of Class II fragments, suggesting that the local environment of ditercalinium affects its conformation.

## Discussion

### Asymmetry and dynamics

DNA-ditercalinium complexes are intrinsically asymmetric. This asymmetry is favored by the dual ring system. Preferences for (i) chair conformations; (ii) equatorial positions of substituents; (iii)  $60_2,180_2$  rotamers combine to impose an approximately  $180^\circ$  difference in the directions of the two N-H bonds of the linker. When the proton of one linker nitrogen forms a hydrogen bond with the DNA and is directed toward the DNA, the proton of the other is directed toward the solvent region. Therefore, hydrogen bonds with the DNA can form with either one linker nitrogen or the other, but not readily with both.

The asymmetry of the DNA-ditercalinium complex results in a degenerate ground state. The orientation of the linker can reverse by net rotation about its long axis (Fig. 2). Upon such ring reversal, the linker nitrogen that initially forms a hydrogen bond to the DNA is redirected toward the solvent. Similarly the linker nitrogen that is initially directed toward the solvent is redirected toward the floor of the major groove to establish a hydrogen bond with the DNA.

The mechanism of ring reversal is somewhere between two limiting possibilities. The first possibility is by dissociation of the intercalated complex, rotation of the linker about its long axis (or end-for-end rotation of the entire molecule), and reassociation with the DNA. The second possibility is by rotation of the linker about its long axis within the bound state. This second possibility is consistent with experimental results. The lifetime of the

bound state is long (around 1 s).<sup>18</sup> NMR line broadening of linker-proton NMR resonances<sup>12</sup> is consistent with lifetimes of each ring orientation that are much less than 1 s.

Certain linker conformations would facilitate ring reversal within the bound state. Ring reversal may be initiated by independent 120° rotation of a single ring (torsion angle  $\gamma$ ) as shown in Figure 6. This rotation of  $\gamma$ , upon slight adjustment of positions of both rings, leads to an intermediate (a 60<sub>3</sub>180<sub>1</sub> rotamer, Fig. 6, middle), stabilized by hydrogen bonds between each linker nitrogen atom and the DNA. A structure-based model of this intermediate is shown in Figure 7A. From the intermediate, rotation of the second ring by 120° restores the more stable 60<sub>2</sub>180<sub>2</sub> rotamer and completes the ring reversal.

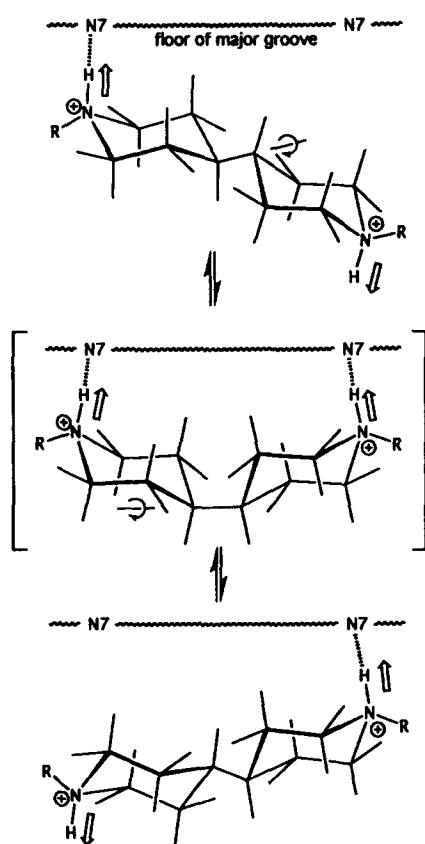


**Figure 6.** Ring reversal pathway in the bound state. The N-7 atoms of guanine are indicated, one of which forms a hydrogen bond to the linker in the ground state. The intercalative groups and connecting ethylene groups are represented by R. Arrows indicate the direction of linker N-H bonds. Linker protons labeled by up arrows form hydrogen bonds to the major groove of the DNA. Rotation of one ring (with its linker proton initially directed away from the DNA) about the central bond of the dual piperidinium ring system by 120° yields the intermediate. Subsequent rotation of the other ring yields the second isoenergetic ground state.

The intermediate can be achieved without serious disturbance of the intercalative moieties, and is expected to be only nominally less stable than the ground state (i.e. the observed 3-D structure of the DNA-ditercalinium complex). The intermediate rotamer (60<sub>3</sub>180<sub>1</sub>) is observed, although less frequently than the 60<sub>2</sub>180<sub>2</sub> rotamer, in dual six-membered rings in the CSD. Furthermore, the

intermediate is stabilized by hydrogen bonds between ditercalinium and DNA and lacks unfavorable steric interactions (modeling, unpublished).

Many aspects of the dual ring system are invariant in the series of fragments found in the CSD. This invariance indicates that the geometry is highly constrained and that the conformations observed in the CSD are relaxed and unperturbed, not artifactual, crystal lattice-induced states.

From an analysis of X-ray structures of bis-intercalated complexes, we have formulated a series of testable hypotheses. We have proposed: (1) a novel mechanism by which antitumor agents can bend DNA;<sup>11</sup> (2) that localized destabilization (inferred from unstacking of DNA bases) could increase the deformability of DNA;<sup>9,10</sup> (3) that the activity of ditercalinium in *E. coli* is caused by excessive or unusual deformability of its DNA complexes;<sup>9,10</sup> (4) that the (A)BC exonuclease repair system recognizes damaged DNA by its excessive or unusual deformability; (5) that specific conformational restraints of the linker of ditercalinium lead to intrinsic asymmetry in its DNA complexes; (6) that ditercalinium complexes are dynamic, converting between degenerate states; (7) that the unique activity of ditercalinium in mammalian systems is related to structural polymorphism and dynamic conversion between conformers.

#### DNA bis-intercalation

As demonstrated by the ditercalinium complex, bis-intercalation can distort DNA in ways that cannot be predicted by summing the effects of two mono-intercalation events. In complexes of triostin A and echinomycin<sup>19,20</sup> some of the base pairs are in Hoogsteen rather than Watson-Crick base pairing arrangements. Although Hoogsteen base pairing may not predominate under all conditions in these complexes in solution,<sup>21</sup> Triostin A clearly increases the relative stability of the Hoogsteen arrangement.

Similarly DNA binding can distort bis-intercalator conformation. The linker of ditercalinium is flexionally stressed in the DNA complex, differing significantly from the consensus conformation derived from the CSD. Each of the dual ring systems found in the CSD is linear while that of ditercalinium is curved (Fig. 7B) and compressed along its long axis. The C-20-C-20' distance is considerably less in ditercalinium than in dual ring systems found in the CSD. This curvature and compression of ditercalinium may arise from an imposition by the DNA of coplanarity of the two chromophores of ditercalinium.

#### Methods

Three-dimensional structures of two types of molecules were extracted from the Cambridge Structural Database (CSD) (5.07, April 1994) with the program QUEST.<sup>14</sup> Class I fragments (Fig. 3A) contain a single ring system and Class II fragments (Fig. 3B) contain dual ring

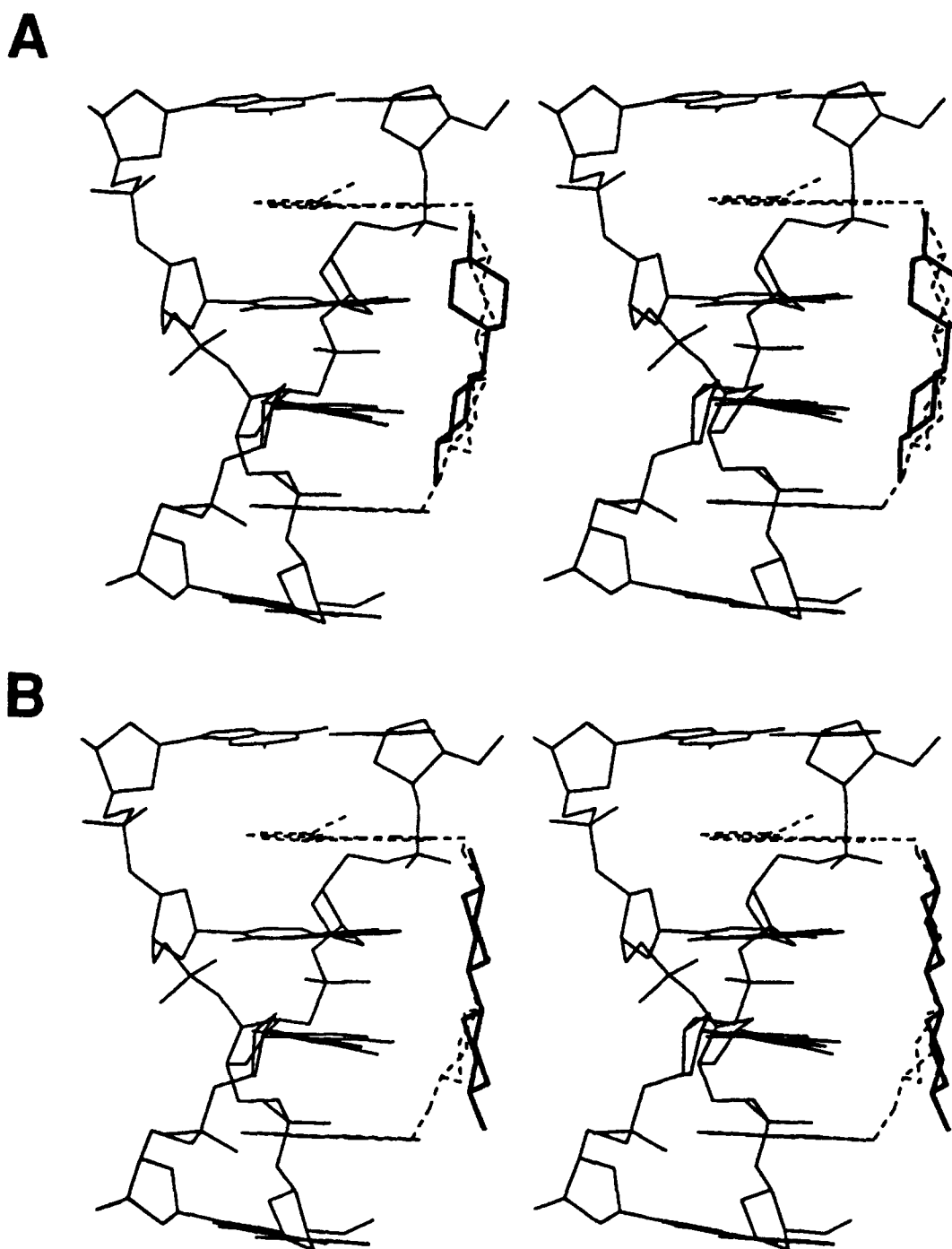


**Figure 7.** Stereo diagrams of the ditercalinium-[d(CGCG)]<sub>2</sub> complex. Ditercalinium bis-intercalates into the DNA via the major groove. DNA is shown in thin lines and ditercalinium in dashed lines. Dual cyclohexane rings, in bold lines, are superimposed on the linker of ditercalinium. Thus, carbon atoms in each model are analogous to nitrogen atoms in the linker. (A) A Class II fragment (CSD entry SOVBAG) was converted to the 60<sub>3</sub>,180<sub>1</sub> rotamer using the program CHAIN<sup>22</sup> to form the intermediate in the ring reversal pathway. This CSD entry was used because its C-20–C-20' distance is closest to the average of all five Class II fragments. C-20–C-20' atoms in the model were docked onto the corresponding atoms of the linker. The fragment was rotated such that the linker nitrogen atoms would be equidistant from and in hydrogen bonding range of the N-7 positions of guanines on the DNA. (B) The uppermost ring of a CSD Class II fragment (entry SOVBAG) was superimposed onto a corresponding ring of ditercalinium.

systems. The ring system of a Class I fragment is defined as a mono-substituted cyclohexane or piperidinium ring. The ring is linked to an acyclic methylene group via the NC atom (see Fig. 3A). One substituent of the methylene group is the previously defined cyclohexane/piperidinium ring system and the other is unrestricted.

The ring systems of Class II fragments are dual, analogous to the linker of ditercalinium. However the linker nitrogen atoms of ditercalinium are replaced by nitrogen or carbon atoms. Each ring is linked to a methylene group via the NC atom (see Fig. 3B) and no other substituents are allowed on the ring system. The second substituent of

each methylene group is left unrestrained. Note that Class I is not a subset of Class II.

Three-dimensional coordinates of each Class I and II entry within the CSD were extracted. Entries are excluded if (i) coordinates are not present; (ii) the  $\sigma_{C-C}$  is greater than 0.04 Å; (iii) the crystallographic *R*-factor is greater than 7%; or (iv) flagged with error or disorder. With these conditions, the CSD contains 47 Class I fragments and five Class II fragments. Geometric analysis was performed with the program GSTAT.<sup>14</sup> Molecules were displayed on a Silicon Graphics Indigo II workstation with the program CHAIN.<sup>22</sup>

### Acknowledgment

This work was funded by the American Cancer Society, Grant NP-831.

### References

- Atwell, G. J.; Stewart, G. M.; Leupin, W.; Denny, W. A. *J. Am. Chem. Soc.* **1985**, *107*, 4335.
- Gaugain, B.; Barbet, J.; Oberlin, R.; Roques, B. P.; Le Pecq, J. B. *Biochemistry* **1978**, *17*, 5071.
- Pelaprat, D.; Delbarre, A.; Le Guen, I.; Roques, B. P.; Le Pecq, J. B. *J. Med. Chem.* **1980**, *23*, 1336.
- Roques, B. P.; Pelaprat, D.; Le Guen, I.; Porcher, G.; Gosse, C.; Le Pecq, J. B. *Biochem. Pharmacol.* **1979**, *28*, 1811.
- Lambert, B.; Roques, B. P.; Le Pecq, J. B. *Nucleic Acids Res.* **1988**, *3*, 1063.
- Lambert, B.; Segal-Bendirdjian, E.; Roques, B. P.; Le Pecq, J.-B. In: *DNA Repair Mechanisms and Their Biological Implications in Mammalian Cells*, pp. 639-652, Lambert, M. W.; Laval, J., Eds; Plenum Press; New York, 1988.
- Lambert, B.; Jones, B. K.; Roques, B. P.; Le Pecq, J. B.; Yeung, A. T. *Proc. Natl Acad. Sci. U.S.A.* **1989**, *86*, 6557.
- Lambert, B.; Segal-Bendirdjian, E.; Esnault, C.; Le Pecq, J. B.; Roques, B. P.; Jones, B.; Yeung, A. T. *Anti-Cancer Drug Design* **1990**, *5*, 43.
- Gao, Q.; Williams, L. D.; Egli, M.; Rabinovich, D.; Chen, S.-H.; Quigley, G. J.; Rich, A. *Proc. Natl Acad. Sci. U.S.A.* **1991**, *88*, 2422.
- Williams, L. D.; Gao, Q. *Biochemistry* **1992**, *31*, 4315.
- Peek, M. E.; Lipscomb, L. A.; Bertrand, J. A.; Gao, Q.; Roques, B. P.; Garbay-Jaureguiberry, C.; Williams, L. D. *Biochemistry* **1994**, *33*, 3794.
- Pothier, J.; Delepierre, M.; Barsi, M. C.; Garbay-Jaureguiberry, C.; Igolen, J.; Le Bret, M.; Roques, B. P. *Biopolymers* **1991**, *31*, 1309.
- Garbay-Jaureguiberry, C.; Laugaa, P.; Delepierre, M.; Laalami, S.; Muzard, G.; Le Pecq, J. B.; Roques, B. P. *Anti-Cancer Drug Design* **1987**, *1*, 323.
- Allen, F. H.; Davies, J. E.; Galloy, J. J.; Johnson, O.; Kennard, O.; Macrae, C. F.; Mitchell, E. M.; Mitchell, G. F.; Smith, J. M.; Watson, D. G. *J. Chem. Info. Comp. Sci.* **1991**, *31*, 187.
- Nasipuri, D. *Stereochemistry of Organic Compounds: Principles and Applications*, John Wiley; New York, 1991.
- Bucourt, R. In: *Topics in Stereochemistry*, Vol. 8, pp. 159-224, Eliel, E. L.; Allinger, N. L., Eds; John Wiley; New York, 1974.
- Testa, B. *Principles of Organic Stereochemistry*, Marcel Dekker; New York, 1979.
- Delepierre, M.; Delbarre, A.; Langlois d'Estaintot, B.; Igolen, J.; Roques, B. P. *Biopolymers* **1987**, *26*, 981.
- Wang, A. H.-J.; Ughetto, G.; Quigley, G. J.; Hakoshima, T.; van der Marel, G. A.; van Boom, J. H.; Rich, A. *Science* **1984**, *225*, 1115.
- Quigley, G. J.; Ughetto, G.; van der Marel, G. A.; van Boom, J. H.; Wang, A. H.-J.; Rich, A. *Science* **1986**, *232*, 1255.
- Gilbert, D. E.; van der Marel, G. A.; van Boom, J. H.; Feigon, J. *Proc. Natl Acad. Sci. U.S.A.* **1989**, *86*, 3006.
- Sack, J. *Chain: A Crystallographic Modelling Program*, Baylor College of Medicine; Waco, TX, 1990.

(Received in U.S.A. 18 October 1994; accepted 19 December 1994)